An improved closed loop hybrid phase shift controller for dual active bridge converter

S. Narasimha[1], Surender Reddy Salkuti[2]
[1]Department of Electrical and Electronics Engineering, TKR College of Engineering and Technology, India
[2]Department of Railroad and Electrical Engineering, Woosong University, Republic of Korea

Article Info	ABSTRACT
	In this paper, a new closed loop hybrid phase shift control is proposed for dual active bridge (DAB) converter with variable input voltage. The extended phase shift (EPS) control is applied when load gets heavy enough and the secondary side phase shift angle decreases to zero. When this modified DAB converter operates at light loads, the triple phase shift (TPS) modulation method is applied, and the added control freedom is the secondary phase shift angle between the two-secondary side switching legs. The hybrid phase shift control (HPS) scheme is a combination of EPS and TPS modulations, and it provides a very simple closed form implementation for the primary and secondary side phase shift angles. Depending on the application by changing the phase shift angles we can achieve Buck or Boost operation. A characteristic table feedback control method has been used for closed loop operation. By using 1D look up table the proposed DAB converter provides constant 400V for any given input voltage.

Corresponding Author:

Surender Reddy Salkuti,
Department of Railroad and Electrical Engineering,
Woosong University,
17-2, Woosong University, Jayang-dong, Dong-gu, Daejeon-34606, Republic of Korea.
Email: surender@wsu.ac.kr

1. INTRODUCTION

In recent years, the isolated bidirectional dc-dc converters (IBDCs) have been used for electric vehicles, microgrids and energy storage systems. Among various invented IBDC topologies, the dual active bridge (DAB) converter has attracted many researchers because of its excellent performance of high-power density, high efficiency, galvanic isolation, buck/boost operation, bidirectional power transfer capability, and modularity. The single phase-shift (SPS) modulation is simple and easy to implement, hence it is commonly employed in many applications. However, the soft-switching range is limited with SPS, and the backflow power or reactive power is also high. The enhanced phase-shift methods are generally named as pulse width modulation plus phase-shift control. To achieve the best performance of the DAB converter over a wide operating range, several modulation methods are combined and hybrid phase-shift (HPS) schemes are introduced. When considering minimum inductor current for a short dead time interval, even larger parts of the theoretical zero voltage sequence (ZVS) region involve the incomplete commutation due to the parasitic output capacitance of MOSFETs, leading to degraded performance and reduced efficiency. However, most of the control schemes presented in the literature on DAB converter only consider the theoretical ZVS constraint, i.e., the inductor current at the switching instant should be of the right polarity (either positive or negative) [1].

To achieve practical ZVS of all switches, a commutation inductor is utilized by decreasing the magnetizing inductance or placing an external inductor between the two phase-leg midpoints in a full

bridge, thereby, generating an enough inductive current to charge and discharge the parasitic output capacitances. The additional commutation inductance current is uncontrolled, and processed by power MOSFETs. An adaptive inductor is used as the main power transfer element such that practical ZVS operation can be achieved at light loads, and the conduction losses are minimized at heavy loads as well. However, the voltage conversion ratio is limited as unity one and the adaptive inductor increases the complexity of implementation. By using the variable-frequency phase-shift control, the soft-switching range can be reduced. But, the wide frequency variation increases design complexity of passive components.

A new closed loop HPS control for a DAB converter with variable input voltage is proposed in reference [1]. The dead time effect has become major aspect in the development of isolated bidirectional full bridge DC-DC converter (IBDC). The theoretical analysis and experimental verification of dead time effect in IBDC has been presented in [2]. Nowadays, high-frequency link (HFL) power conversion systems (PCSs) are attracting more and more attentions in academia and industry because of their high power density, reduced weight, and low noise. The core circuit of DAB IBDC is HFL PCSs, and basic strategy of control, soft-switching solution are described in reference [3]. In reference [4], an improved dual output dc-dc converter is proposed in which the duty cycle is regulated by pulse width modulation. This improved converter preserves all the advantages of its original version: both outputs can be fully regulated without additional switches. A high voltage DC bus in a fuel cell car as a bidirectional electrical interface between 12V battery and DAB is proposed in [5].

In reference [6], the conventional phase shift and triangular current modulations are compared in terms of the power transfer and total loss. To reduce switching and conduction losses, the optimal switching frequency designed. Here, a hybrid modulation strategy with variable switching frequency is proposed to reduce the losses and to increase the performance. The soft switching range by bidirectional LLC circuit with new control methods for all the switches is proposed in [7]. The transient response of a DAB DC-DC converter by using two different phase shift methods are presented in reference [8]. Here, a modified asymmetric double-side modulation is proposed to minimize the transient time. Buck and boost operating modes are enabled in DAB converters which enables the bidirectional power flow is proposed in [9]. Analysis of reactive power loss and high efficiency of novel optimization method and modulation solution for IBDC DAB proposed in [10], operates over a wide input range, and the switching losses are reduced and ZVS range has increased.

The first step towards maximizing the performance of an IBDC is to review the limitations of existing systems. The major losses in power electronics are switching losses. By using single phase shift modulation, the soft switching range is limited. The extended phase shift (EPS) modulation is applied when the load is heavy and the triple phase shift (TPS) modulation applied for light loads. The zero voltage sequence (ZVS) region is limited and switching losses are more. A novel closed loop hybrid phase shift (HPS) control scheme is developed for a dual active bridge converter with variable input voltage. The extended phase shift (EPS) control is applied when the load gets heavy enough and the secondary side phase shift angle decreases to zero [11-12]. When this modified DAB converter operates at light loads, the triple phase shift (TPS) modulation method is applied, and the added control freedom is the secondary phase shift angle between the two-secondary side switching legs. Both buck and boost operation MATLAB Simulink circuits have been executed for EPS and TPS modulations and the input pulses, output voltage and power Simulink results has been described for input voltage range of (200-400)V.

2.   DIFFERENT PHASE SHIFT CONTROL TECHNIQUES FOR DAB CONVERTERS

In several engineering applications, it is needed to convert a fixed voltage DC supply into a variable voltage DC supply. A DC-DC converter, converts directly from DC to DC and is just called a DC converter. A DC converter can be considered as DC corresponding to associate AC electrical device with an incessantly variable turn's magnitude relation. Sort of an electrical device, it will be accustomed step down or step up a DC voltage supply. Control strategy is one of the important research directions for DAB-isolated bidirectional full bridge DC-DC converter (IBDC) [13]. The control strategies for dual active bridge (DAB) converters are introduced and analyzed in this section, and they are presented next:

2.1. Single phase shift (SPS) control

This is the most widely used control method for Dual active bridge (DAB) - Isolated bidirectional dc-dc converter (IBDC). Only a phase-shift ratio (or angle) D can be controlled. Then, the power flow direction and magnitude can be controlled easily. SPS control is beneficious due to small inertia, and ease of realizing soft-switching control. Moreover, the converter cannot operate under zero voltage sequence (ZVS) in the whole power range. Therefore, the power loss becomes much higher, and its efficiency is greatly reduced [14].

2.2. Extended phase shift (EPS) control

EPS control is a typically improved method of SPS control. The output ac voltage of one bridge becomes a three-level wave while the another one is a two-level 50% square wave. Compared with SPS control, the operating states of two bridges will be same when the voltage conversion states or power flow directions are changed. Hence, the EPS control is easier to implement, and has better dynamic performance [15].

2.3. Triple phase shift (TPS) control

The triple phase modulation is employed when the converter operates at light loads. The TPS modulation is employed such that the practical ZVS operation can be extended to zero [16]. Hence, TPS control is easier to implement, and its dynamic performance is excellent.

2.4. Hybrid phase shift (HPS) modulation

The HPS modulation is a combination of EPS and TPS modulations. It provides a simple closed form implementation for the primary and secondary side phase shift angles. This HPS modulation has the advantages of EPS and TPS modulations [17].

3.   PROPOSED CIRCUIT TOPOLOGY

In this paper, a center tapped transformer (CTT) based DAB converter is proposed, by inserting a small inductor (L_s) between the transformer center tap and the mid-point of split output capacitors (C'_{s1} and C'_{s2}) in the conventional DAB converter topology [18, 19]. Here, the two-inductor CTT based DAB converter is used and it is shown in Figure 1(a). The turns ratio of CTT is $N_1:N_2 = N_1:N_3 = n$. A T-type and a Δ-type primary-referred equivalent circuits of modified DAB converter are derived with the equivalent transformation of transformer and impedance. The magnetizing inductance (L_m) of CTT is neglected in this analysis and transformation, due to the fact that L_m is larger than the phase-shift inductors [20].

The CTT associated with two phase-shift inductors driven by three ac voltages are u_1, u'_2 and u'_3. CTT-based ac equivalent can be directly derived, as shown in Figure 1(a). By replacing the phase-shift inductor L'_s with two equal inductors (L'_2 and L'_3) connected in series with the secondary windings, the CTT-based ac equivalent circuit with three phase-shift inductors are derived and shown in Figure 1(b). The values of the three inductors that are used in this model are expressed as [21, 22],

$$L_1 = L_p - L'_s \tag{1}$$

$$L'_2 = 2L'_s \tag{2}$$

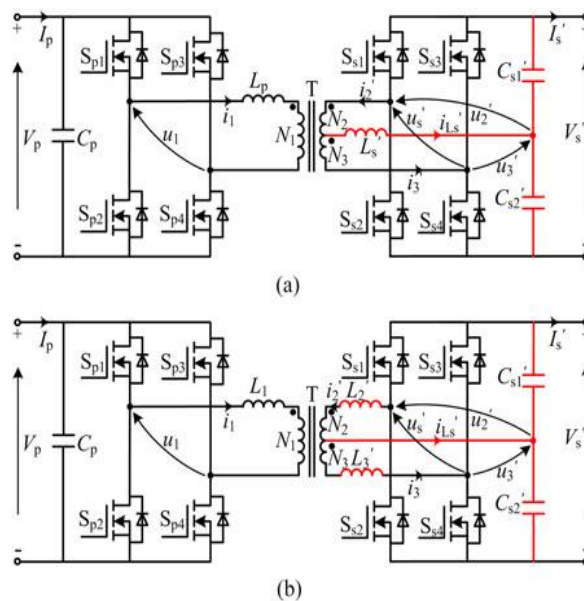$$L'_3 = 2L'_s \tag{2}$$

(a)

(b)

Figure 1. Proposed CTT based DAB converter topologies with (a) two inductors and (b) three inductors

Mode 1 operation is considered as an example to explore the operation of modified DAB converter with the Extended phase shift (EPS) control, and due to the symmetry, only three stages over the half switching are described.

3.1. TPS modulation

To extend the ZVS range, the TPS modulation is applied, and the added control freedom is the phase-shift angle ($\emptyset_s$). For the sake of shortening control and analysis, phase-shift angle ($\emptyset_s$) is expected to be better than or equal to zero always. Figure 2 depicts the equivalent circuits of modified DAB converter with TPS control. Depending on the sequence in time of the dropping and rising edges of u_1 and u_s, six operating modes for bidirectional power flow can be identified. Modes 1 and modes 4 exist both in forward and reverse power flows, whereas modes 2 and modes 3 occur only in the forward power flow, and modes 2B and modes 3B exist in the reverse power transfer [23].
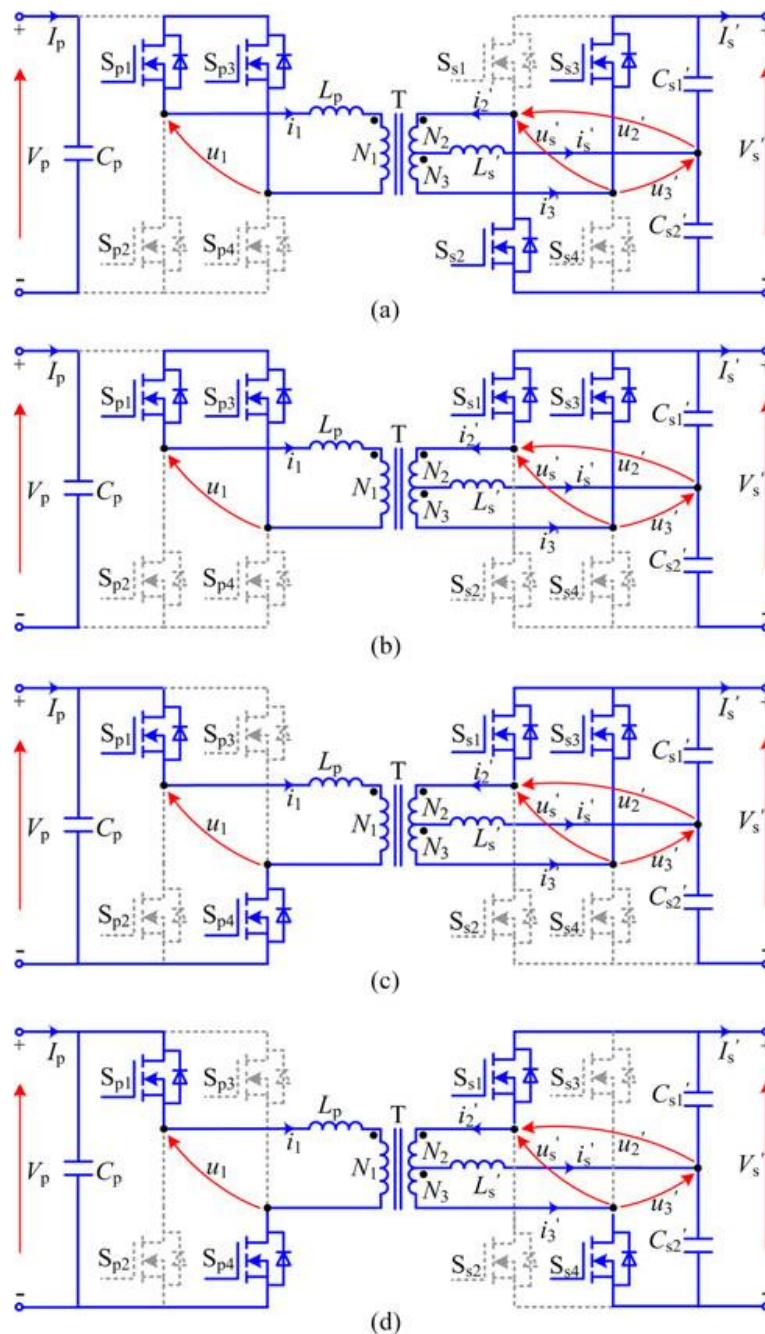

Figure 2. Equivalent circuits of modified DAB converter with TPS control

3.2. HPS control strategy

For high-voltage MOSFETs, low currents ($0<I_{ZVS}<2A$) are insufficient to recharge the parasitic drain-to-source capacitance within a 200ns dead time interval, leading to increased switching losses. Therefore, $I_{ZVS}=2A$ is adopted as the practical ZVS condition. To simplify the following analysis and design, the transformer turns ratio $N_1:N_2:N_3$ is assumed as 1:1:1. Here, the worst switching current (i_{wst}) and worst switching leg for each operating mode under TPS have been identified. To enable the practical ZVS operation of all power transistors, the practical ZVS condition for the worst switches should be satisfied. The primary-secondary phase-shift angle (φ) is used to act the main control, variable regulating the output voltage (V_s), and the other two phase-shift angles φ_p and φ_s are utilized to maximize the efficiency performance [24-25]. The HPS control scheme applied to the modified DAB converter is depicted in Figure 3.
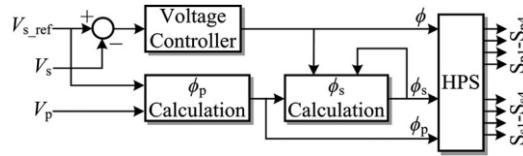

Figure 3. HPS control scheme applied to the modified DAB converter

When the transferred power is relatively low, the HPS controlled converter is modulated with TPS. When the power is large enough, φ_s decreases to 0, and the converter is EPS modulated [26]. Which means that the transmission power is independent of the phase-shift angle φ_s, but is mainly dominated by the phase-shift angle φ. This is beneficial to decoupling the regulation of output voltage (V_s) and the realization of practical ZVS operation. On the other hand, the addition of φ_s can assist all power switches to achieve practical ZVS; thereby, significantly minimizing the switching losses. Therefore, the HPS control is superior over the EPS control.

4. RESULTS AND DISCUSSION

In this paper, depending on the application, by changing the phase shift angles, one can achieve buck/boost operation. MATLAB Simulink software is used for investigating both EPS and TPS modulations for different operating modes of buck and boost operations. Here, four modes of operations are performed. For each mode of operation, MATLAB simulation circuit, output voltage and power waveforms are provided [27]. In Mode 1 operation, buck operation wave forms are presented. In Mode 2 and Mode 3 operations, boost operation wave forms are presented. In Mode 4, again buck operation wave forms are presented. By using the EPS control method, Mode 1 operation will give the buck operation. Figure 4 depicts the switching pulses applied to the power electronic devices.
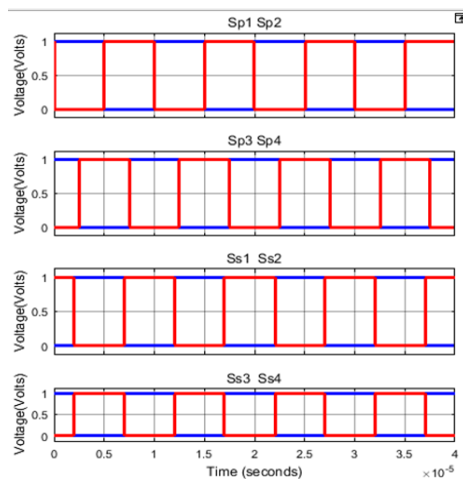

Figure 4. Switching pulses applied to power electronic devices

Figure 5 depicts the output voltage in buck mode operation (i.e., Mode 1). For the given input voltage of 400V, the obtained output voltage is 375V, and this can be seen from Figure 5. Figure 5 also shows the output power in buck mode operation with EPS control (i.e., Mode 1 operation). For the given input voltage of 400V, the obtained output power is 878W, and it can be seen from Figure 5.
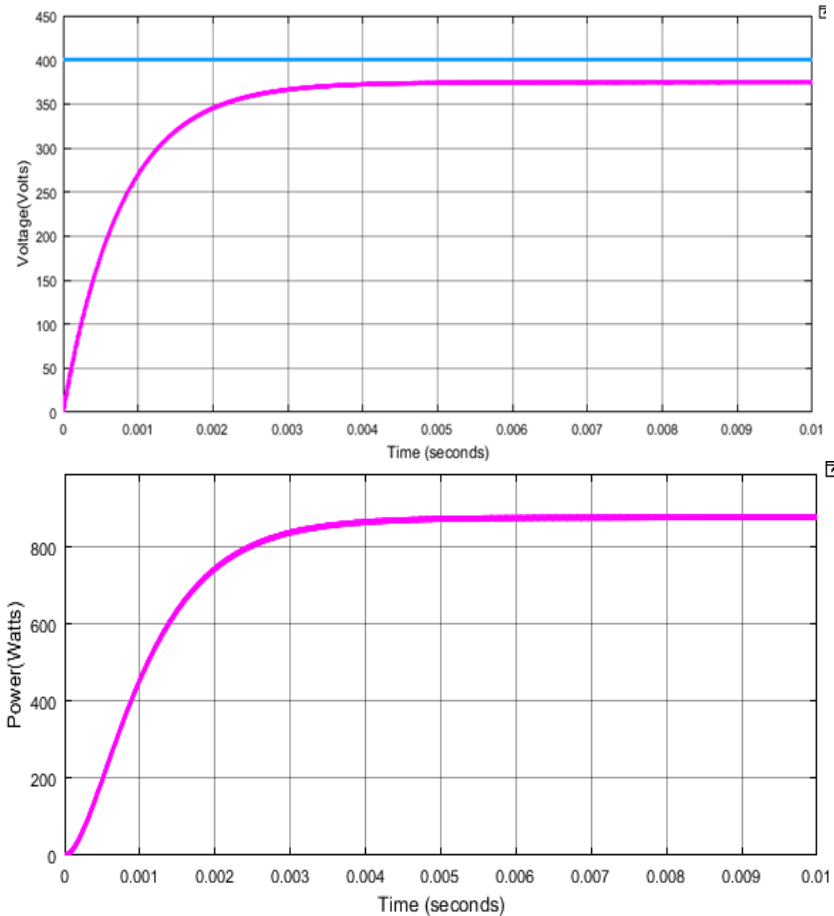

Figure 5. Output voltage and output power of the converter with EPS control (in Mode 1) for the input voltage of 400V

4.1. TPS Control Approach

In Mode 2 operation, S_{s1} and S_{s4} are turned ON and this interval ends up with S_{p3} being switched OFF. In Mode 3 operation, S_{s1} is triggered ON and this interval ends up with S_{p1} being switched OFF. In TPS control method (i.e., Mode 2), the boost operation will give 543V output voltage for a given input voltage of 200V. Then, the output power is 1881W. Figure 6 depicts the output voltage of converter with TPS control boost operation (i.e., Mode 2 operation). For the given input voltage of 400V, the obtained output voltage is 1087V, and this can be observed in Figure 6. Figure 6 also shows the output power of the converter in boost (i.e., Mode 2) operation with TPS control. For the given input voltage of 400V, the obtained output power is 7385W, and it can be observed in Figure 6.

Figure 7 presents the output voltage of the converter in boost operation (Mode 3). For the given input voltage of 400V, the obtained output voltage is 596V. Figure 7 also depicts the output power of the converter in boost operation (i.e., Mode 3). For the given input voltage of 400V, the obtained power output is 2225W. Figure 8 depicts the output voltage of the converter in buck operation (i.e., Mode 4 operation). For the given input voltage of 400V, the obtained output voltage is 154V, and it can be seen from Figure 8. Figure 8 also depicts the output power of the converter in buck operation (i.e., Mode 4). For the given input voltage of 400V, the obtained power output is 148W.
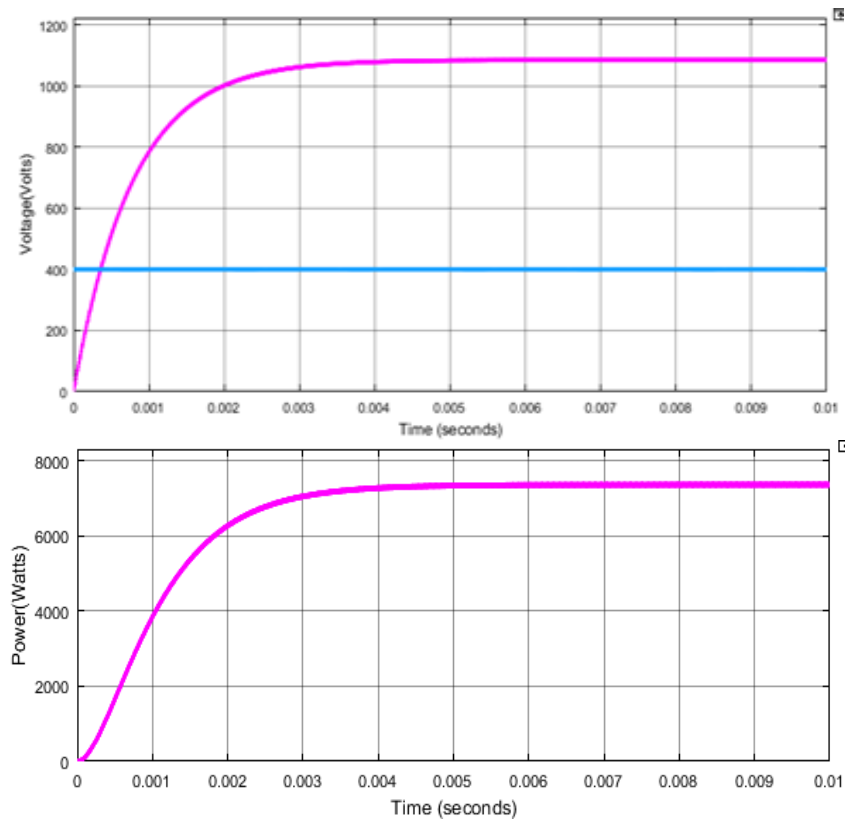
Figure 6. Output voltage and power of the converter with TPS control (Mode 2) for the input voltage of 400V
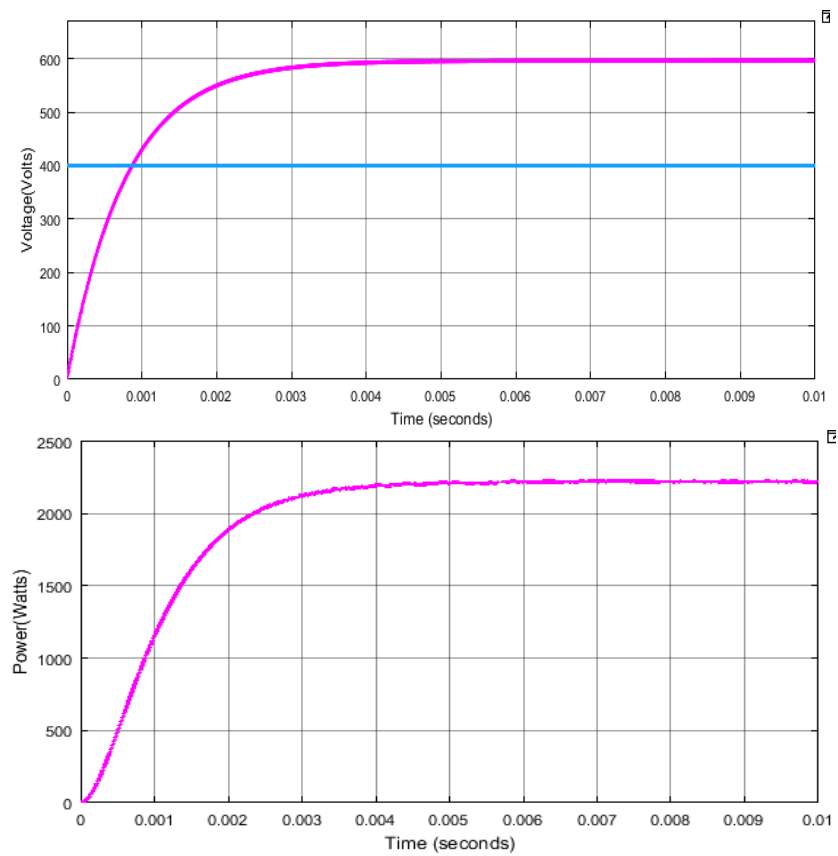

Figure 7. Output voltage and power of the converter (i.e., Mode 3) for the input voltage of 400V
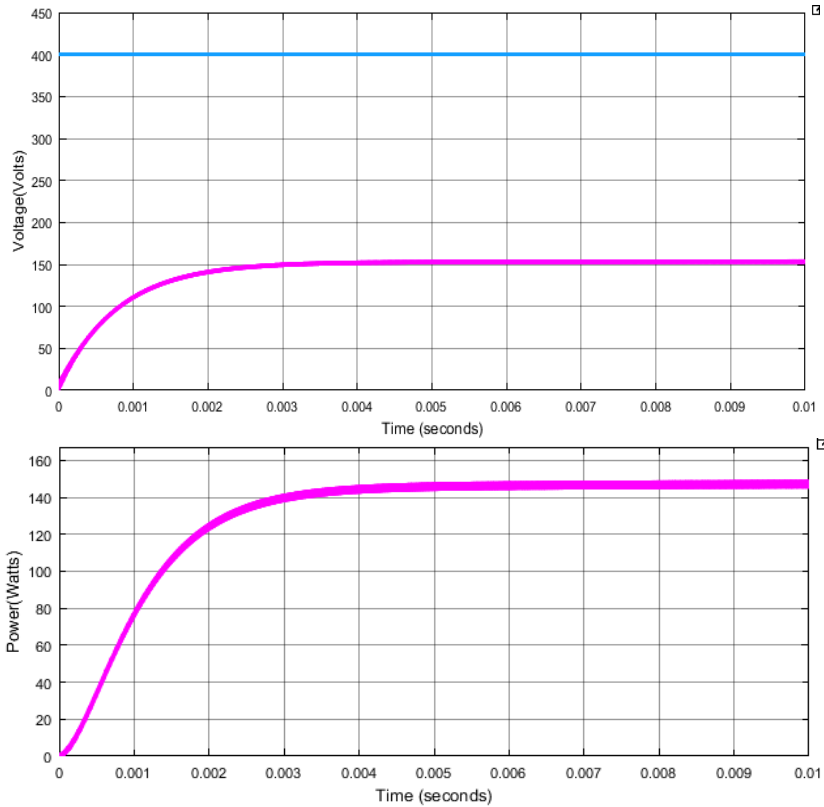
Figure 8. Output voltage and power of the converter (i.e., Mode 4) for the input voltage of 400V

4.2. Hybrid phase shift (HPS) feedback control structure with characteristic table

The HPS control scheme is a combination of EPS and TPS modulations. By using the feedback control with characteristic table method, the phase shift required to get 400V output voltage for any given input voltage in the range of (200-400)V is calculated, by using 1D lookup table. The table data contains time break points (1e-6, 6e-6, 4e-6, 2e-6, 1e-6) and voltage break points (200V, 250V, 300V, 350V and 400V), which are calculated by using trial and error method. For any given input voltage range of (200-400)V, the phase shift time is calculated and applied to get 400V constant output voltage. The output voltage waveforms without closed loop feedback and with closed loop feedback control of characteristic table method are compared in this section. The ripple factor has been reduced by using the feedback control. Figure 9 depicts the comparison of output voltage with and without the feedback control.
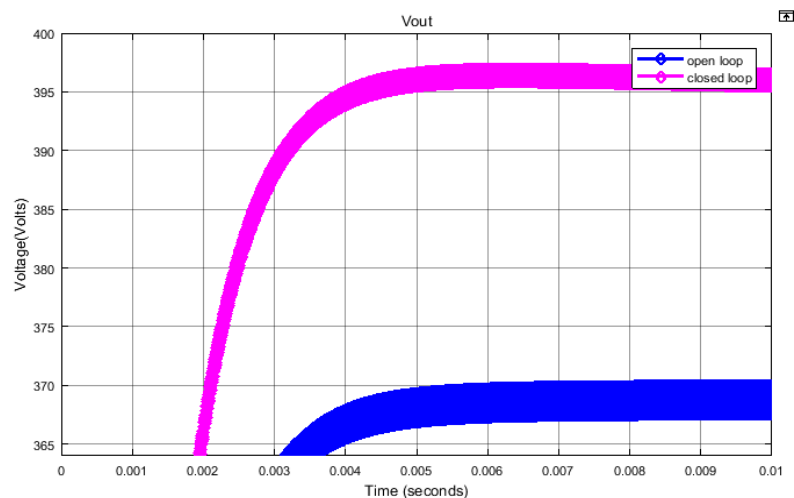

Figure 9. Comparison of output voltage waveforms for with and without the feedback control

Ripple factor is defined as,

$$Ripple\ Factor = \frac{V_{max} - V_{min}}{V_{max}} * 100 \qquad (4)$$

Ripple factor without feedback is calculated as,

$$Ripple\ Factor = \frac{370 - 367}{370} * 100 \ = \ 0.8\% \qquad (5)$$

Ripple factor with characteristic table closed loop feedback control is calculated as,

$$Ripple\ Factor = \frac{397 - 395}{397} * 100 \ = 0.5\% \qquad (6)$$

From the above (5) and (6), it is clear that the ripple factor without feedback is 0.8% and the with feedback is 0.5%. From this, it can be observed that the ripple factor has been reduced significantly with characteristic table closed loop feedback control. Table 1 presents the comparison of output voltage and power values for the given input voltage of 400V. In the Table, Mode 1 represents the buck operation, Modes 2 and Modes 3 represents the boost operations, Mode 4 represents the buck operation.

Table 1. Comparison of output voltage and power in four modes

Mode of operation	For $V_{in} = 400V$	
	V_{out}	P_{out}
Mode1	$375V$	$878W$
Mode2	$1087V$	$7385W$
Mode3	$597V$	$2225W$
Mode4	$154V$	$149W$

5. CONCLUSION

In this paper, a novel modified dual active bridge (DAB) converter and a simple HPS control scheme for a 0.5-1 variation in the voltage conversion ratio is proposed. The HPS control scheme is a combination of EPS and TPS modulations, and it provides a very simple closed-form implementation for the primary and secondary side phase shift angles. When this modified DAB converter operates at light loads, the TPS modulation is employed such that the practical ZVS operation can be extended to zero load. For heavy loads, the secondary side phase shift angle decreases to zero, and the EPS modulation is applied. By using the 1D look up table, the proposed dual active bridge (DAB) converter provides constant 400V for any given input voltage range of (200-400)V and the ripple factor has been reduced from 0.8% to 0.5%.

REFERENCES

[1] Y. Shen, X. Sun, W. Li, X. Wu, and B. Wang, "A Modified Dual Active Bridge Converter With Hybrid Phase-Shift Control for Wide Input Voltage Range," *IEEE Transactions on Power Electronics*, vol. 31, no. 10, pp. 6884-6900, 2016.
[2] B. Zhao, Q. Song, W. Liu, and Y. Sun, "Dead-Time Effect of the High-Frequency Isolated Bidirectional Full-Bridge DC–DC Converter: Comprehensive Theoretical Analysis and Experimental Verification," *IEEE Transactions on Power Electronics*, vol. 29, no. 4, pp. 1667-1680, 2014.
[3] B. Zhao, Q. Song, W. Liu, and Y. Sun, "Overview of Dual-Active-Bridge Isolated Bidirectional DC-DC Converter for High-Frequency-Link Power-Conversion System," *IEEE Transactions on Power Electronics*, vol. 29, no. 8, pp. 4091-4106, 2014.
[4] Y. Chen, and Y. Kang, "An Improved Full-Bridge Dual-Output DC–DC Converter Based on the Extended Complementary Pulse width Modulation Concept," *IEEE Transactions on Power Electronics*, vol. 26, no. 11, pp. 3215-3229, 2011.

[5]   F. Krismer and J.W. Kolar, "Accurate Power Loss Model Derivation of a High-Current Dual Active Bridge Converter for an Automotive Application," *IEEE Transactions on Industrial Electronics*, vol. 57, no. 3, pp. 881-891, 2010.

[6]   X.F. He, Z. Zhang, Y.Y. Cai and Y.F. Liu, "A Variable Switching Frequency Hybrid Control for ZVS Dual Active Bridge Converters to Achieve High Efficiency in Wide Load Range," *IEEE Applied Power Electronics Conference and Exposition, Fort Worth, TX, USA*, 2014, pp.1095-1099.

[7]   T. Jiang, J. Zhang, X. Wu, K. Sheng and Y. Wang, "Bidirectional LLC Resonant Converter with Automatic Forward and Backward Mode Transition," *IEEE Transactions on Power Electronics*, vol. 30, no. 2, pp. 757-770, 2015.

[8]   X. Li and Y.F. Li, "An Optimized Phase-Shift Modulation for Fast Transient Response in a Dual-Active-Bridge Converter," *IEEE Transactions on Power Electronics*, vol. 29, no. 6, pp. 2661-2665, 2014.

[9]   G.G. Oggier and M. Ordonez, "High Efficiency DAB Converter Using Switching Sequences and Burst-Mode," *IEEE Transactions on Power Electronics*, vol. 31, no. 3, pp. 2069-2082, 2016.

[10] H. Wen, W. Xiao and B. Su, "Non-active Power Losses Minimization in a Bidirectional Isolated DC-DC Converter for Distributed Power System", *IEEE Transactions on Industrial Electronics*, vol. 61, no. 12, pp. 6822-6831, 2014.

[11] P. Gupta and A. Patra, "Hybrid sliding mode control of DC-DC power converter circuits," *TENCON Conference on Convergent Technologies for Asia-Pacific Region*, Bangalore, India, 2003, pp. 259-263.

[12] A. Safari and H. Ardi, "Sliding Mode Control of a Bidirectional Buck/Boost DC-DC Converter with Constant Switching Frequency," *Iranian Journal of Electrical and Electronic Engineering*, vol. 14, no. 1, pp. 69-84, 2018.

[13] D.D. Nguyen, D.H. Nguyen, T. Funabashi and G. Fujita, "Sensorless Control of Dual-Active-Bridge Converter with Reduced-Order Proportional-Integral Observer," *Energies*, vol. 11, no. 4, pp. 1-18, 2018.

[14] Y. Zhang, X. Li, C. Sun and Z. He, "Improved Step Load Response of a Dual-Active-Bridge DC-DC Converter," *Electronics*, vol. 7, pp. 1-15, 2018.

[15] A. Rodríguez, A. Vázquez, D.G. Lamar, M.M. Hernando, J. Sebastián, "Different purpose design strategies and techniques to improve the performance of a Dual Active Bridge with phase-shift control," *IEEE 15th Workshop on Control and Modeling for Power Electronics (COMPEL)*, Santander, 2014, pp. 1-10.

[16] A. Kumar, A.H. Bhat and P. Agarwal, "Review and comparative analysis of dual active bridge isolated DC to DC converter with different control techniques," *International Journal of Industrial Electronics and Drives*, vol. 4, no. 2, pp. 69-84, 2018.

[17] N. Hou, W. Song, Y. Zhu, X. Sun and W. Li, "Dynamic and static performance optimization of dual active bridge DC-DC converters," *Journal of Modern Power Systems and Clean Energy*, vol. 6, no. 3, pp. 607-618, 2018.

[18] R. Sowmya and S. Rama Reddy, "Comparison of PI & Fuzzy Logic Controlled Dual Active Bridge DC to DC Converter Systems," *International Journal of Electrical & Computer Sciences*, vol. 15, no. 3, pp. 21-29, 2015.

[19] J. Li, D. Wang, W. Wang and J. Jiang, "Minimize Current Stress of Dual-Active-Bridge DC-DC Converters for Electric Vehicles Based on Lagrange Multipliers Method," *Energy Procedia*, vol. 105, pp. 2733-2738, 2018.

[20] C. Bai, B. Han and M. Kim, "Current-fed dual-half-bridge converter directly connected with half-bridge inverter for residential photovoltaic system," *Solar Energy*, vol. 174, pp. 108-120, 2018.

[21] R.O. Núñez, G.G. Oggier, F. Botterón and G.O. García, "A comparative study of Three-Phase Dual Active Bridge Converters for renewable energy applications," *Sustainable Energy Technologies and Assessments*, vol. 23, pp. 1-10, 2017.

[22] Z. Xuan, H. Shenghua and N. Guoyun, "A Three-phase Dual Active Bridge Bidirectional ZVS DC/DC Converter," *Physics Procedia*, vol. 24(A), pp. 139-148, 2012.

[23] S.S. Muthuraj, V.K. Kanakesh, P. Das and S.K. Panda, "Triple Phase Shift Control of an LLL Tank Based Bidirectional Dual Active Bridge Converter," *IEEE Transactions on Power Electronics*, vol. 32, no. 10, pp. 8035-8053, 2017.

[24] M. Ahmed, A. Elhassane and A. Mohamed, "Modelling and Passivity-based Control of a Non Isolated DC-DC Converter in a Fuel Cell System," *International Journal of Electrical and Computer Engineering (IJECE)*, vol. 8, no. 5, pp. 3436-3443, 2018.

[25] E. Setiawan, T. Hirata and I. Hodaka, "Accurate Symbolic Steady State Modeling of Buck Converter," *International Journal of Electrical and Computer Engineering (IJECE)*, vol. 7, no. 5, pp. 2374-2381, 2017.

[26] S.N. Rao, D.V. Ashok Kumar and C.S. Babu, "Grid Connected Distributed Generation System with High Voltage Gain Cascaded DC-DC Converter Fed Asymmetric Multilevel Inverter Topology," *International Journal of Electrical and Computer Engineering (IJECE)*, vol. 8, no. 6, pp. 4047-4059, 2018.

[27] S. Narasimha and S.S. Reddy, "Dynamic and Hybrid Phase Shift Controller for Dual Active Bridge Converter," *International Journal of Engineering & Technology*, vol. 7, no. 4, pp. 4795-4800, 2018.